

Demixing in mesoscopic boson-fermion clouds inside cylindrical harmonic traps: Quantum phase diagram and role of temperature

Z. Akdeniz,^{1,2} A. Minguzzi,¹ P. Vignolo,¹ and M. P. Tosi¹¹*NEST-INFM and Scuola Normale Superiore, Piazza dei Cavalieri 7, I-56126 Pisa, Italy*²*Department of Physics, University of Istanbul, Istanbul, Turkey*

(Received 27 February 2002; published 30 July 2002)

We use a semiclassical three-fluid model to evaluate the phenomena of spatial demixing in mesoscopic clouds of fermionic and bosonic atoms at high dilution under harmonic confinement. We assume repulsive boson-boson and boson-fermion interactions and include a bosonic thermal cloud at finite temperature T . The finite system size allows three different regimes for the equilibrium density profiles at $T=0$: a fully mixed state, a partially mixed state in which the overlap between bosons and fermions is decreasing, and a fully demixed state where the two clouds have zero overlap. We propose simple analytical rules for the two crossovers between the three regimes as functions of the system parameters and support these rules by extensive numerical calculations. A universal “phase diagram” is shown to be valid for the transition to the regime of full demixing, where we identify several exotic configurations in addition to simple ones consisting of a core of bosons enveloped by fermions and vice versa. With increasing temperature some exotic configurations are transformed into more symmetric ones, until demixing is ultimately lost. For very high values of the boson-fermion repulsion we also report demixing between the fermions and the thermally excited bosons.

DOI: 10.1103/PhysRevA.66.013620

PACS number(s): 03.75.Fi, 05.30.-d, 73.43.Nq, 67.40.Kh

I. INTRODUCTION

After the realization of Bose-Einstein condensation (BEC) in atomic gases [1], one of the most challenging endeavours in experiments on cold atoms is the cooling of fermionic isotopes of alkali atoms down to the expected superfluid transition. Theoretical estimates based on the BCS model [2] indicate that the temperature for the superfluid transition should be much lower than the Fermi temperature T_f , which is of the order of the BEC transition temperature. In fact, cooling fermions is harder than cooling bosons: the main difficulty arises from Fermi statistics, as s -wave collisions between spin-polarized fermions in a magnetic trap are forbidden by the Pauli principle. A common strategy uses sympathetic cooling, which is based on s -wave collisions between the fermions and a second gaseous component made either of fermions in a different internal state or of bosons. The latter choice seems to minimize the effects of Pauli blocking, which limit the process of cooling two fermionic components [3]. Several experiments are currently in progress on trapping and cooling various boson-fermion mixtures, i.e., ^6Li - ^7Li [4,5], ^6Li - ^{23}Na [6], and ^{40}K - ^{87}Rb [7]. The lowest temperature attained in these experiments so far is about $0.2T_f$.

From the theoretical point of view a mixture of condensed bosons and fermions in the normal state is already an interesting system to study, because it can show spatial demixing of the two components [8]. In the homogeneous gas at $T=0$ this is an example of a quantum phase transition, that is a phase transition induced by the interactions [9]: on increasing the boson-fermion repulsion the system minimizes its total energy by placing the bosons and the fermions (or boson-fermion mixtures of different compositions) in different regions of space [10], even though this implies a high cost of kinetic energy at the interface. Examples of boson-

fermion demixing in a quasispherical trap have been given by Nygaard and Mølmer [11], while the conditions for demixing inside a spherical trap have been set out by two of us [12] for $N_b=N_f$ and by Miyakawa *et al.* [13] for $N_f \ll N_b$, with N_b and N_f the numbers of bosons and fermions in the trap. The conditions for observing demixing in the Paris experiment on a ^6Li - ^7Li mixture in a cigar-shaped trap [5] have been analyzed by Akdeniz *et al.* [14]. There are, of course, important consequences of finite system size and inhomogeneity of the external confinement on demixing in trapped mixtures, relative to the case of a homogeneous one. In particular, the transition is spread out in a finite system and the anisotropy of the trap acts differently on the two types of atoms (expressions such as phase transition and phase diagram will nevertheless continue to be used for brevity in the following). Locating the onset of partial demixing is also relevant to the practicalities of fermion cooling, since at that point the diminishing overlap between the two clouds will start reducing the effectiveness of the collisional transfer.

In this paper we complement the previous works on boson-fermion mixtures [8–14] by giving the general conditions under which phase separation can occur in a harmonic trap in terms of the physical parameters of the system (for arbitrary values of the anisotropy parameter, scattering lengths, numbers of bosons and fermions, atomic masses and trapping frequencies). We also treat demixing under confinement at finite temperature. To locate the region of phase separation at zero temperature we draw a universal phase diagram expressed in terms of two scaling parameters of the system. Our analysis is supported by an extensive study of the equilibrium density profiles of the bosonic and fermionic components within a mean-field model, ranging from a fully mixed state at small values of the scattering lengths to the partially demixed state at intermediate values of the coupling constants and finally to the regime of full phase separation. In the phase-separated regime we find several configurations

having different symmetry and topology, some of which are metastable, and investigate the role of the anisotropy of the confinement in determining the minimum-energy configurations. We then consider the boson-fermion mixture at finite temperature, finding that on increasing temperature some phase-separated configurations turn or decay into others of higher symmetry before phase separation disappears. Finally, we show that phase separation between the fermions and a bosonic thermal cloud is also possible, in principle, on further increase of the boson-fermion scattering length.

The paper is organized as follows. In Sec. II we describe the model that we have used and give the limits of its applicability, together with a schematic description of the numerical method employed to find the phase-separated configurations. Section III summarizes the conditions under which phase separation occurs at $T=0$, illustrates various configurations that can be found in the phase-separated regime and gives the phase diagram for the lowest-energy configurations. Section IV illustrates the effect of temperature on the configurations obtained for both small and large boson-fermion scattering length. Finally, Sec. V gives a summary and some concluding remarks.

II. THE METHOD

We describe the boson-fermion mixture by means of the particle density profiles, which are $n_c(\mathbf{r})$ for the condensate, $n_{nc}(\mathbf{r})$ for the bosonic thermal cloud, and $n_f(\mathbf{r})$ for the fermions. The components are subject to axially symmetric confining potentials given by

$$V_{b,f}^{ext}(\mathbf{r}) = m_{b,f} \omega_{b,f}^2 (r_\perp^2 + \lambda_{b,f}^2 z^2) / 2, \quad (1)$$

where $m_{b,f}$ are the atomic masses, $\omega_{b,f}$ the trap frequencies, and $\lambda_{b,f}$ the trap anisotropies. We evaluate the density profiles in a mean-field model using the Thomas-Fermi approximation for the condensate and the Hartree-Fock approximation for the other clouds.

The Thomas-Fermi approximation assumes that the number of condensed bosons is large enough that the kinetic-energy term in the Gross-Pitaevskii equation may be neglected [15]. It yields

$$n_c(\mathbf{r}) = [\mu_b - V_b^{ext}(\mathbf{r}) - 2gn_{nc}(\mathbf{r}) - fn_f(\mathbf{r})] / g \quad (2)$$

for positive values of the function in the square brackets and zero otherwise. Here, μ_b is the chemical potential of the bosons and the coupling constants are $g = 4\pi\hbar^2 a_{bb}/m_b$ and $f = 2\pi\hbar^2 a_{bf}/m_r$, with a_{bb} and a_{bf} the boson-boson and boson-fermion scattering lengths and $m_r = m_b m_f / (m_b + m_f)$ the reduced mass. The Hartree-Fock approximation [16–18], on the other hand, treats the thermal boson cloud and the fermion cloud as ideal gases subject to effective potentials $V_{b,f}^{eff}$, that is,

$$n_{nc,f}(\mathbf{r}) = \int \frac{d^3p}{(2\pi\hbar)^3} \times \left\{ \exp \left[\left(\frac{p^2}{2m_{b,f}} + V_{b,f}^{eff}(\mathbf{r}) - \mu_{b,f} \right) / k_B T \right] \mp 1 \right\}^{-1}, \quad (3)$$

where

$$V_b^{eff}(\mathbf{r}) = V_b^{ext}(\mathbf{r}) + 2gn_c(\mathbf{r}) + 2gn_{nc}(\mathbf{r}) + fn_f(\mathbf{r}) \quad (4)$$

and

$$V_f^{eff}(\mathbf{r}) = V_f^{ext}(\mathbf{r}) + fn_c(\mathbf{r}) + fn_{nc}(\mathbf{r}). \quad (5)$$

The chemical potentials $\mu_{b,f}$ characterize the system in the grand-canonical ensemble and are determined by requiring that the volume integrals of the densities $n_c(\mathbf{r}) + n_{nc}(\mathbf{r})$ and $n_f(\mathbf{r})$ should be equal to the average numbers N_b and N_f of particles.

The mean-field model is valid for the bosons when the diluteness condition $n_c a_{bb}^3 \ll 1$ holds and the temperature is not very close to the transition temperature (outside the critical region). The fermionic component has been taken as a dilute spin-polarized gas, for which the fermion-fermion s -wave scattering processes are inhibited by the Pauli principle and p -wave scattering is negligible [19]. The condition $k_f a_{bf} \ll 1$ with k_f the Fermi wave number should hold in the mixed regime, but this is not a constraint in the regime of phase separation where the boson-fermion overlap is rapidly dropping. With regard to the thermal cloud, no significant differences have been found between the predictions of the Hartree-Fock and Popov approximations in the regime $n_c a_{bb}^3 \ll 1$, except at very low temperatures where the thermal cloud is becoming negligible [20]. For the specific case of trapped atomic vapors, the semiclassical Hartree-Fock approximation has also been tested by a Monte Carlo calculation [21], performed with a choice of parameters appropriate to the ^{87}Rb gas.

The density profiles at fixed numbers N_b and N_f are determined numerically by a self-consistent solution of the above equations. The profiles are obtained in two self-consistency loops: first, Eqs. (2) and (3) are solved at fixed chemical potentials starting from some initial guesses for the densities; then the chemical potentials are found iteratively by a standard algorithm for multivariable root finding for the normalization equations that fix the number of bosons and fermions. Whereas in the mixed state the density profiles at convergence do not depend on the initial choice, different configurations are found in the phase-separation regime for the same values of the parameters by varying the initial conditions. We have used this fact to search for several possible metastable configurations, which will be illustrated in Sec. III B below.

III. PHASE DIAGRAM AT ZERO TEMPERATURE

As is evident from the preceding section, a boson-fermion mixture under confinement is characterized by a large number of parameters. The aim of this section is to analyze what is the effect of varying them independently and to provide a unified understanding of the results using scaling laws.

The interaction energy grows on increasing the values of the boson-boson and boson-fermion coupling constants. There exists a threshold beyond which the total energy is minimized by a configuration in which the two components are spatially separated. The transition to the phase-separated

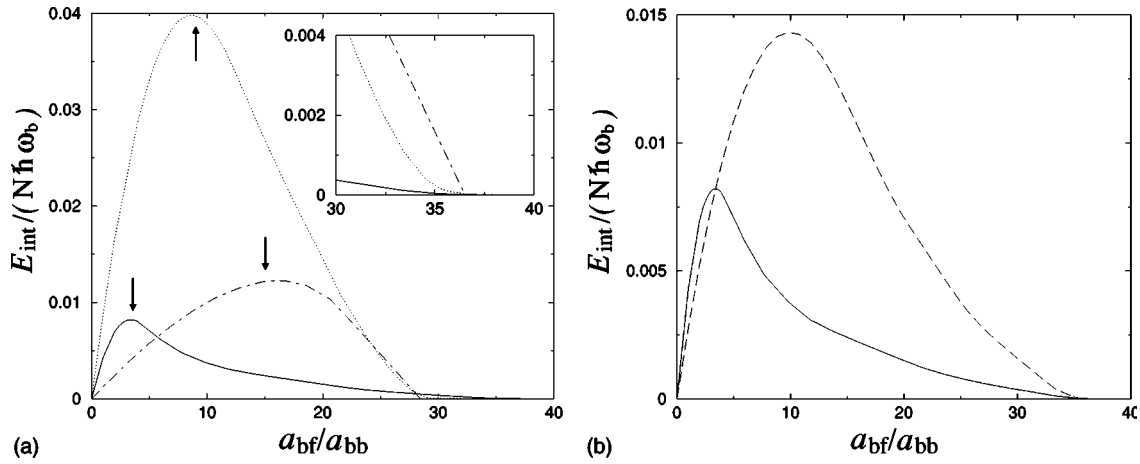


FIG. 1. Boson-fermion interaction energy at $T=0$ (in units of $N\hbar\omega_b$ where $N=N_f+N_b$) as a function of the adimensional ratio a_{bf}/a_{bb} for $a_{bb}=5.1a_0$ with a_0 being the bohr radius. The other parameters are $\omega_b/2\pi=4000$ Hz, $\omega_f/2\pi=3520$ Hz, $\lambda_b\approx\lambda_f\approx 1/60$, and atomic masses corresponding to the ${}^6\text{Li}$ - ${}^7\text{Li}$ mixture. (a) For $N=2.1\times 10^5$, with $N_{f,1}=10^4$ (continuous line), $N_{f,2}=1.05\times 10^5$ (dotted line), and $N_{f,3}=2\times 10^5$ (dotted-dashed line). The arrows indicate the positions of the maxima according to Eq. (7). In the inset are shown the same curves in the same vertical units, after rescaling the second and third curves along the horizontal axis by factors $(N_{f,2}/N_{f,1})^{1/12}$ and $(N_{f,3}/N_{f,1})^{1/12}$. (b) For a fixed number of fermions $N_f=10^4$ and different numbers of bosons $N_b=2\times 10^5$ (continuous line) and $N_b=10^4$ (dashed line).

regime is smooth owing to the finite size of the confined gas, and three different states are indeed recognizable: mixed, partially demixed, and fully demixed. Depending on the value of the relative strength of the two coupling constants, it may happen that either the fermions or the bosons are pushed away from the center of the trap.

A. Partial demixing

The boson-fermion interaction energy is proportional to the overlap between bosonic and fermionic clouds and at $T=0$ we have

$$E_{int} = f \int d^3r n_b(\mathbf{r}) n_f(\mathbf{r}). \quad (6)$$

We locate the onset of partial demixing by looking at the point where the boson-fermion overlap starts to decrease with increasing a_{bf}/a_{bb} .

In the following we focus on the simplest case where only one scattering length is varied, which also seems realistic from an experimental point of view. Then the most efficient way to approach phase separation is by changing a_{bf} (see Sec. III B below). The behavior of the interaction energy as a function of the ratio a_{bf}/a_{bb} at fixed a_{bb} is shown in Fig. 1(a).

The position of the maximum of the interaction energy at fixed a_{bb} can be estimated analytically from the condition $\partial E_{int}/\partial f=0$, by using the approximate expressions $n_{b,f} \approx N_{b,f}/(4\pi R_{b,f}^3/3)$ and the values for the cloud radii R_f and R_b as obtained in the absence of boson-fermion interactions, $R_f=(48N_f/\lambda_f)^{1/6}a_f$ and $R_b=(15\lambda_b N_b a_{bb}/a_b)^{1/5}a_b/\lambda_b^{1/3}$ with $a_{b,f}=(\hbar/m_{b,f}\omega_{b,f})^{1/2}$. The expression for the position of the maximum is

$$\left. \frac{a_{bf}}{a_{bb}} \right|_{max} = \left(c_1 \frac{N_f^{1/2}}{N_b^{2/5}} + c_2 \frac{N_b^{2/5}}{N_f^{1/3}} \right)^{-1}, \quad (7)$$

where

$$c_1 = \frac{15^{3/5}}{48^{1/2}} \frac{\lambda_f^{1/2}}{\lambda_b^{2/5}} \frac{m_f^{3/2} \omega_f}{2m_r m_b^{1/2} \omega_b} \left(\frac{a_{bb}}{a_b} \right)^{3/5} \quad (8)$$

and

$$c_2 = \frac{48^{1/3}}{15^{3/5}} \left(\frac{6}{\pi} \right)^{2/3} \frac{\lambda_b^{2/5}}{\lambda_f^{1/3}} \frac{m_b \omega_b}{2m_r \omega_f} \left(\frac{a_{bb}}{a_b} \right)^{2/5}. \quad (9)$$

We recognize in Eq. (7) a geometric combination of two scaling parameters: $c_1 N_f^{1/2}/N_b^{2/5}$ is dominant in the case $N_b \ll N_f$ while $c_2 N_b^{2/5}/N_f^{1/3}$ was previously identified [22] in the regime $N_f \ll N_b$. The predictions obtained from Eq. (7) are indicated in Fig. 1(a) by vertical arrows. There clearly is very good agreement between the analytical estimate and the numerical results.

As a final comment, we would like to stress again that partial phase demixing is a peculiarity of the harmonically trapped case. In the homogeneous system a partial overlap between the two species is only restricted to the region of the interface and appears in the calculation if one takes into account the surface kinetic-energy effects [23]. In the trapped system, for large numbers of particles when the Thomas-Fermi approximation is valid, we expect that inclusion of the quantum tails in the calculation will produce only small modifications of the semiclassical profiles and of the behavior of the interaction energy shown in Fig. 1.

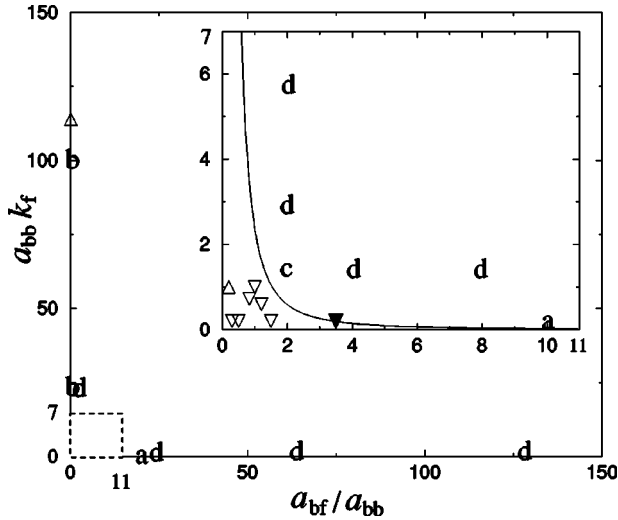


FIG. 2. Phase diagram at $T=0$, in the plane defined by the adimensional parameters $a_{bb}k_f$ and a_{bf}/a_{bb} . The bottom left corner of the figure is shown enlarged in the inset. The continuous line in the inset corresponds to the condition of phase separation given by Eq. (10). In the mixed-phase regime we have the following configurations: \triangle , fermions at the center; ∇ , bosons at the center; \blacktriangledown , bosons at the center in an almost demixed configuration. For the phase-separated regime we have used the following notations (see Fig. 4): (a) symmetric configuration with fermions outside; (b) symmetric configuration with bosons outside; (c) boson torus inside a fermion cloud; (d) three-component symmetric configuration with fermions outside and in the central core. All the configurations in this phase diagram have been evaluated at zero temperature, using $N_b = N_f = 10^4$, $\omega_b/2\pi = 4000$ Hz, $\omega_f/2\pi = 3520$ Hz, $\lambda_b \approx \lambda_f \approx 1/60$, and atomic masses corresponding to the ^6Li - ^7Li mixture.

B. Full demixing

The regime of full demixing is taken to be reached when the boson-fermion overlap becomes negligible. As is shown in Fig. 1(b), within the three-fluid model the transition point does not depend on the number of bosons in the trap. This can also be predicted from the results obtained by Viverit *et al.* [10] for the homogeneous mixture, by using the values of the densities taken at the center of the trap. Within the same approximation for the fermion density as in Sec. III A we obtain the condition for phase separation at $T=0$ as

$$\alpha k_f a_{bb} > \left(\frac{a_{bb}}{a_{bf}} \right)^2, \quad (10)$$

where $k_f = (48\lambda_f N_f)^{1/6}/a_f$ and $\alpha = [3^{1/3}/(2\pi)^{2/3}]m_b m_f / (4m_r^2)$. Equation (10) is valid for different numbers of bosons and fermions as well as for different atomic masses and trap frequencies, and agrees very well with the phase-separation criterion given earlier by two of us [12] for the case where $m_f = m_b$ and $\omega_f = \omega_b$. It confirms that the two relevant parameters for describing the transition to the fully demixed regime are a_{bf}/a_{bb} and $\alpha k_f a_{bb}$. We also immediately find that the value of a_{bf} at the transition point scales as $N_f^{-1/12}$ at fixed a_{bb} : this result is illustrated in the inset in Fig. 1(a).

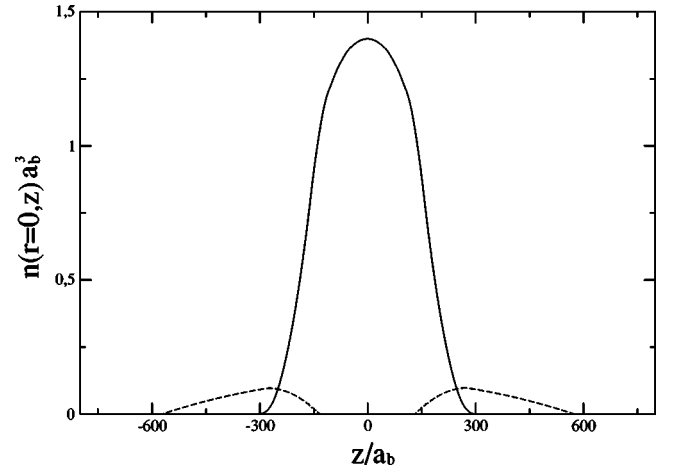


FIG. 3. Section of the density profiles (in units of a_b^{-3}) as a function of z/a_b for fermions (solid line) and bosons (dashed line) in a configuration where a mixed phase and a purely bosonic one coexist (\triangle in Fig. 2). This configuration has been obtained at $T=0$ with $a_{bb} = 323\,000a_0$ and $a_{bf} = 32\,300a_0$. The numbers of atoms and all other parameters are as in Fig. 2.

Equation (10) has been verified by the numerical solution of the three-fluid model for a variety of different sets of parameters. First of all we have studied the location of phase separation in parameter space by varying the scattering lengths over much wider ranges than allowed by the usual off-resonant values (e.g., in the ^6Li - ^7Li mixture), as might be attained experimentally by exploiting optically or magnetically induced Feshbach resonances [24]. For these calculations we have chosen the geometrical parameters of the traps and the numbers of atoms as in the Paris experiment on

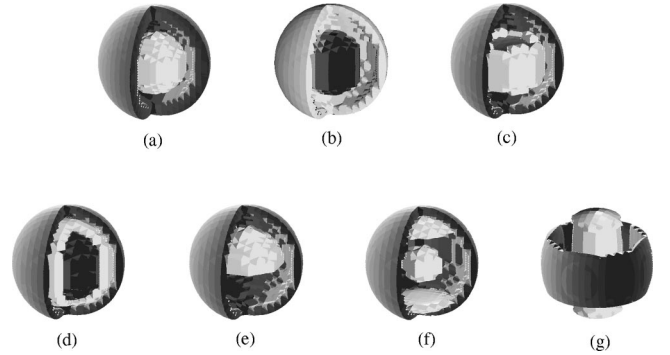


FIG. 4. Configurations in the phase-separated regime for $N_f = N_b = 10^4$ particles at $T=0$. (a) Symmetric configuration with fermions outside; (b) symmetric configuration with bosons outside; (c) boson torus inside fermion cloud; (d) threefold symmetric configuration; (e) asymmetric configuration; (f) boson sandwich inside a fermion cloud; and (g) torus of fermions around an elongated core of bosons. The structures (a) and (c)–(f) are for the same values of $a_{bb} = 600a_0$ and $a_{bf} = 6000a_0$, and their energies per particle are $4.24\hbar\omega_b$, $4.71\hbar\omega_b$, $5.38\hbar\omega_b$, $5.50\hbar\omega_b$, and $5.85\hbar\omega_b$. The configuration (b) was obtained for $a_{bb} = 64\,600a_0$ and $a_{bf} = 32\,300a_0$ and the value of its energy per particle is $13.25\hbar\omega_b$. The configuration (g) was obtained for $a_{bb} = 6250a_0$ and $a_{bf} = 12\,500a_0$ and the value of its energy per particle is $9.27\hbar\omega_b$. All other parameters are as in Fig. 2.

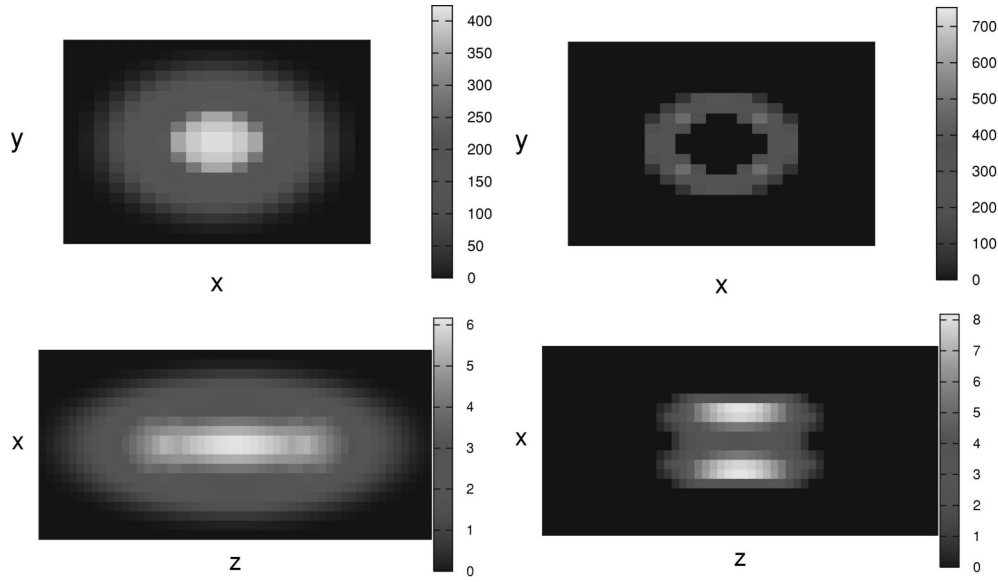


FIG. 5. Column densities (in units of a_b^{-2}) in the radial plane (top) and in the $\{x,z\}$ plane (bottom) for the fermionic cloud (left) and the bosonic cloud (right) of the bosonic torus [configuration (c) in Fig. 4, obtained with $a_{bb}=600a_0$ and $a_{bf}=6000a_0$]. The size of the figures in the $\{x,y\}$ plane and in the $\{x,z\}$ plane is $11 \mu\text{m} \times 11 \mu\text{m}$ and $11 \mu\text{m} \times 400 \mu\text{m}$, respectively. The other parameters are as in Fig. 2.

^6Li - ^7Li [5]: namely, $N_b \approx N_f = 10^4$, $\omega_b/2\pi = 4000$ Hz, $\omega_f/2\pi = 3520$ Hz, and $\lambda_b \approx \lambda_f \approx 1/60$. The results are summarized in a quantum phase diagram at $T=0$ in the plane $\{a_{bf}/a_{bb}, k_f a_{bb}\}$, which is reported in Fig. 2. This contains all the lowest-energy configurations that we have found, with the inset showing an enlargement of the region near the origin of the above-mentioned plane. The curve drawn inside the inset in Fig. 2 is obtained from Eq. (10) and is in full agreement with the numerical results in separating the region of full demixing from the mixing or partial-demixing regions.

We turn to a detailed account of the configurations corresponding to the various symbols and letters in the phase diagram in Fig. 2. Below the phase-separation line in the inset two different types of configurations are found, one with a core of bosons in partial overlap with an envelope of mainly fermions (triangles down) and a specular one with a core of fermions enveloped by mainly bosons (triangle up). An interesting configuration that we have observed in the latter case shows coexistence of a mixed state with a purely bosonic phase (see Fig. 3): this combination is not stable in the homogeneous mixture [10].

In the regime of phase separation a variety of different configurations are observed, including several that require a break of the symmetry imposed by the confining harmonic potentials. The letters $a-d$ in the phase diagram in Fig. 2 give the locations of four such energetically stable structures, which are shown in Fig. 4 together with some other metastable structures. The symmetric configuration with boson inside and fermion outside, indicated by (a), is obtained in Fig. 4 with the choice $a_{bb}=600$ bohr radii and $a_{bf}=10a_{bb}$, while the complementary configuration (b) formed from fermions inside and bosons outside is obtained with $a_{bb}=64\,600$ bohr radii and $a_{bf}=a_{bb}/2$. Other configurations obtained with the same scattering lengths as the symmetric structure of type (a) are shown in Fig. 4: these are (c) a boson torus inside a fermion cloud, (d) a threefold symmetric structure formed from fermions surrounded by a shell of bosons inside a fermion envelope, (e) an asymmetric structure in which the bosons are shifted away from the center of the trap along the z axis, and (f) a “sandwich” formed by bosons inside a fermion cloud. Finally the structure indicated by (g) in Fig. 4, which consists of a torus of fermions around an elongated boson core, is found with the choice $a_{bb}=6250$ bohr radii and $a_{bf}=2a_{bb}$.

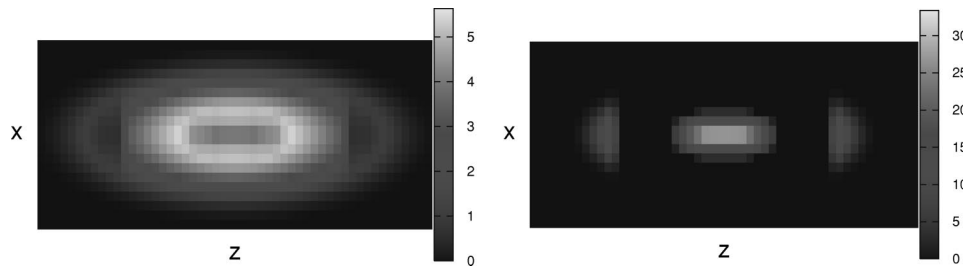


FIG. 6. Column densities in the $\{x,z\}$ plane (in units of a_b^{-2}) for the fermions (left) and for the condensate (right) in the sandwich configuration (f) in Fig. 4, obtained with $a_{bb}=600a_0$ and $a_{bf}=6000a_0$. The size of the figures is $11 \mu\text{m} \times 400 \mu\text{m}$. The other parameters are as in Fig. 2.

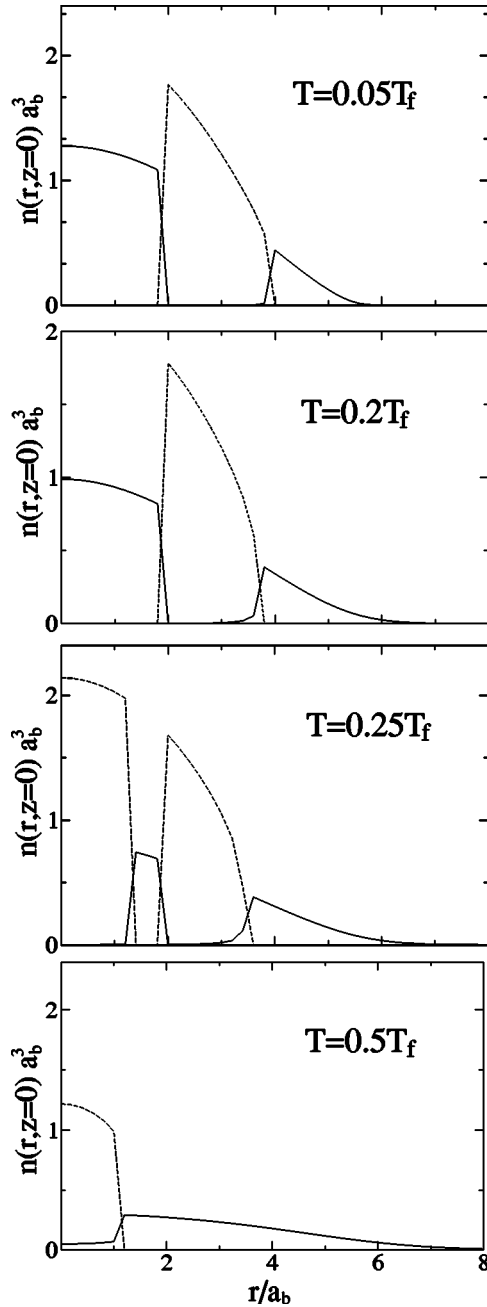


FIG. 7. Sections of the density profiles at different temperatures (in units of a_b^{-3}) for the fermions (solid line) and for the condensate (dashed line) as functions of the radial coordinate r/a_b for the configuration (c) in Fig. 4, obtained with $a_{bb}=600a_0$ and $a_{bf}=6000a_0$. The values of the other parameters are as in Fig. 2.

With the exception of (a) and (b) the configurations shown in Fig. 4 are very different from the density distributions that are met in the mixed phase, and thus could be identified in an experiment by looking at the column-density pictures of the atomic clouds. As an illustration we give in Fig. 5 the column-density images corresponding to the case (c) of a bosonic torus, and in Fig. 6 those for the case (f) of a boson sandwich.

Finally, we have examined the role of the anisotropy of the confinement on the configurations of lowest energy in the

phase-separated regime. To this end we have evaluated the stability of the lowest-energy configuration by varying the anisotropy from $\lambda_f=1/60$ to $\lambda_f=1$ while keeping the ratio $\lambda_b/\lambda_f \approx 1$, with the choice $a_{bb}=600$ bohr radii and $a_{bf}=10a_{bb}$ for the scattering lengths. The most stable configuration remains the symmetric structure (a) except that for $\lambda_f \approx 1$ the structure (d) has the lowest energy. For this particular choice of parameters the relative difference in energy between the metastable configurations does not vary much with λ_f .

IV. THE ROLE OF TEMPERATURE

At finite temperature an increasing fraction of the bosons populates the thermal cloud, thus depleting the condensate. In harmonic confinement the thermal cloud is wider and more dilute than the condensate, and thus is much less interacting with the fermions. As a result the thermal cloud is not yet in phase separation when the condensate already is.

At low temperatures the noncondensate fraction is small and its presence does not affect the description of the phase separation between the condensate and the fermions that we have given in the preceding section. In particular we have verified that at T of the order of $0.2T_f$, as are reached in current experiments, all the exotic configurations (c) to (g) remain possible. They are not found at higher temperatures: we show as an example in Fig. 7 the behavior of the boson torus configuration (c) as a function of temperature. For $0.2T_f < T \leq 0.3T_f$ a part of the condensed bosons moves from the torus to the center of the trap and for $T > 0.3T_f$ the phase separation is lost.

At still higher temperatures the thermal cloud starts to be consistently populated and we have found that phase separation between the fermions and the entire bosonic cloud becomes possible for very large values of a_{bf}/a_{bb} [14]. In this case, as is illustrated in Fig. 8, the fermion cloud exhibits a central hole having the size of the bosonic thermal cloud.

V. SUMMARY AND CONCLUDING REMARKS

We have performed an extensive analysis of the phenomenon of phase separation for a boson-fermion mixture under confinement on the basis of the atomic density profiles of the two components. First of all we have pointed out that three regimes can be identified owing to the inhomogeneity of the external confinement of the system: a mixed phase where the bosonic and fermionic clouds overlap, a partially demixed state where the overlap is decreasing, and a fully phase-separated regime where there is no overlap between the two components at zero temperature. We have given analytical expressions for the positions of the two crossovers between these regimes in terms of the physical parameters of the system, and verified these conditions by an extensive numerical study based on varying the coupling constants, the numbers of atoms, and the geometry of the trap. General expressions for the transition lines are particularly useful in view of the several experiments in progress [5–7], which are run with different experimental parameters such as the relative num-

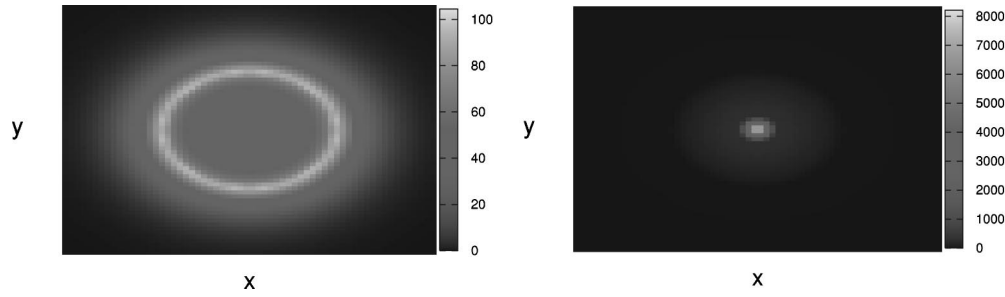


FIG. 8. Column densities in the $\{x,y\}$ plane (in units of a_b^{-2}) for fermions (left) and bosons (right) in the fully demixed regime at $T = 0.6T_f$, for $a_{bb} = 5.1a_0$ and $a_{bf} = 2 \times 10^3 a_0$. The values of the other parameters are as in Fig. 2. In the right panel the thermal bosons are hardly visible because of the high density of the central condensate. The size of the figures is $11 \mu\text{m} \times 11 \mu\text{m}$.

bers of bosons and fermions, the atomic masses, and the trap anisotropies.

The transition to the partially phase-separated regime, that we have located where the boson-fermion interaction energy starts to decrease on increasing the boson-fermion scattering, is important for the experiments on fermion cooling: the boson-fermion collision rate is decreased by a geometrical factor that is proportional to the overlap between the two clouds. At fixed boson-boson scattering length we have given a simple model for the transition in terms of a combination of two scaling parameters, which characterize the cases $N_b \ll N_f$ and $N_f \ll N_b$.

The transition to full demixing has been illustrated by a universal phase diagram expressed in terms of scaling parameters of the system. It is remarkable that in our model the location of this transition does not depend on the number of bosons. In the region of phase separation we have found several configurations with various topology and identified the minimum-energy configurations. We have also investigated the effect of increasing temperature on phase separation. Some exotic configurations that are found in the phase diagram at $T=0$ turn into others of higher symmetry before the condensate-fermion demixing is lost.

In our estimates we have used two robust zero-order (mean-field) approximations, which are known to describe well the main features of harmonically trapped ultradilute atomic gases: the Thomas-Fermi approximation for the con-

densate and the semiclassical Hartree-Fock approximation for the other gaseous clouds, where we have neglected the effects of the surface kinetic energy. The Thomas-Fermi approximation breaks down for a very small condensate or for negative values of the boson-boson scattering length, and one would then need to solve the full Gross-Pitaevskii equation. Inclusion of the quantum levels into the Hartree-Fock approximation leads to the appearance of small shell effects at ultralow temperatures. A description beyond mean field is required when the dilution parameters increase and for a trapped gas this is still an open problem. The analog of the Beliaev expansion at $T=0$ has recently been derived for the homogeneous boson-fermion mixture [25].

Of course, the evolution of the mixture towards phase separation modifies not only its equilibrium properties, but also its dynamical properties and collective excitation spectrum. The approach to the transition will be signalled by a softening of the frequencies of surface or bulk modes having the appropriate symmetry for a phase-separated configuration to be attained. Experiments measuring dynamical properties could therefore provide an alternative method for revealing the onset of demixing. Calculations on these spectra are in progress.

ACKNOWLEDGMENT

This work was supported by INFM through the PRA2001-Photonmatter.

-
- [1] M.H. Anderson, J.R. Ensher, M.R. Matthews, C.E. Wieman, and E.A. Cornell, *Science* **269**, 198 (1995); K.B. Davis, M.-O. Mewes, M.R. Andrews, N.J. van Druten, D.S. Durfee, D.M. Kurn, and W. Ketterle, *Phys. Rev. Lett.* **75**, 3969 (1995); C.C. Bradley, C.A. Sackett, J.J. Tollett, and R.G. Hulet *ibid.* **75**, 1687 (1995).
 - [2] H.T.C. Stoof, M. Houbiers, C.A. Sackett, and R.G. Hulet, *Phys. Rev. Lett.* **76**, 10 (1996).
 - [3] B. DeMarco, S.B. Papp, and D.S. Jin, *Phys. Rev. Lett.* **86**, 5409 (2001).
 - [4] A.G. Truscott, K.E. Strecker, W.I. McAlexander, G.B. Partridge, and R.G. Hulet, *Science* **291**, 2570 (2001).
 - [5] F. Schreck, L. Khaykovich, K.L. Corwin, G. Ferrari, T. Bourdel, J. Cubizolles, and C. Salomon, *Phys. Rev. Lett.* **87**, 080403 (2001).
 - [6] Z. Hadzibabic, C.A. Stan, K. Dieckmann, S. Gupta, M.W. Zwierlein, A. Görlitz, and W. Ketterle, *Phys. Rev. Lett.* **88**, 160401 (2002).
 - [7] J. Goldwin, S.B. Papp, B. DeMarco, and D.S. Jin, *Phys. Rev. A* **65**, 021402(R) (2002).
 - [8] K. Mølmer, *Phys. Rev. Lett.* **80**, 1804 (1998).
 - [9] S.L. Sondhi, S.M. Girvin, J.P. Carini, and D. Shahar, *Rev. Mod. Phys.* **69**, 315 (1997).
 - [10] L. Viverit, C.J. Pethick, and H. Smith, *Phys. Rev. A* **61**, 053605 (2000).
 - [11] N. Nygaard and K. Mølmer, *Phys. Rev. A* **59**, 2974 (1999).
 - [12] A. Minguzzi and M.P. Tosi, *Phys. Lett. A* **268**, 142 (2000).
 - [13] T. Miyakawa, K. Oda, T. Suzuki, and H. Yabu, *J. Phys. Soc. Jpn.* **69**, 2779 (2000).

- [14] Z. Akdeniz, P. Vignolo, A. Minguzzi, and M.P. Tosi, J. Phys. B **35**, L105 (2002).
- [15] G. Baym and C.J. Pethick, Phys. Rev. Lett. **76**, 6 (1996).
- [16] A. Minguzzi, S. Conti, and M.P. Tosi, J. Phys.: Condens. Matter **9**, L33 (1997).
- [17] M. Amoruso, A. Minguzzi, S. Stringari, M.P. Tosi, and L. Vichi, Eur. Phys. J. D **4**, 261 (1998).
- [18] P. Vignolo, A. Minguzzi, and M.P. Tosi, Phys. Rev. A **62**, 023604 (2000).
- [19] B. DeMarco, J.L. Bohn, Jr., J.P. Burke, M. Holland, and D.S. Jin, Phys. Rev. Lett. **82**, 4208 (1999).
- [20] F. Dalfovo, S. Giorgini, and S. Stringari, Rev. Mod. Phys. **71**, 463 (1999).
- [21] M. Holzmann, W. Krauth, and M. Narachewski, Phys. Rev. A **59**, 2956 (1999).
- [22] L. Vichi, M. Amoruso, A. Minguzzi, S. Stringari, and M.P. Tosi, Eur. Phys. J. D **11**, 335 (2000).
- [23] P. Ao and S.T. Chui, Phys. Rev. A **58**, 4836 (1998).
- [24] S. Inouye, M.R. Andrews, J. Stenger, H.-J. Miesner, D.M. Stamper-Kurn, and W. Ketterle, Nature (London) **392**, 151 (1998); S.L. Cornish, N.R. Claussen, J.L. Roberts, E.A. Cornell, and C.E. Wieman, Phys. Rev. Lett. **85**, 1795 (2000).
- [25] A.P. Albus, S.A. Gardiner, F. Illuminati, and M. Wilkens, Phys. Rev. A **65**, 053607 (2002).